

A MEEVC discretization for two-dimensional incompressible Navier-Stokes equations with general boundary conditions

Yi Zhang^{a,*}, Artur Palha^b, Marc Gerritsma^b, Qinghe Yao^c

^aUniversity of Twente, Drienerlolaan 5, 7522 NB, Enschede, the Netherlands

^bDelft University of Technology, Mekelweg 5, 2628 CD, Delft, the Netherlands

^cSun Yat-sen University, Gongchang road 66, 518107, Shenzhen, China

Abstract

In this work, we introduce a mass, energy, enstrophy and vorticity conserving (MEEVC) mixed finite element discretization for two-dimensional incompressible Navier-Stokes equations as an alternative to the original MEEVC scheme proposed in [A. Palha and M. Gerritsma, J. Comput. Phys., 2017]. The present method can incorporate no-slip boundary conditions. Conservation properties are proven. Supportive numerical experiments with both exact and inexact quadrature are provided.

Keywords: Navier-Stokes equations, de Rham complex, structure-preserving discretization, no-slip boundary condition

1. Introduction

We consider the dimensionless rotational or Lamb form of two-dimensional incompressible (or, more strictly speaking, constant density) Navier-Stokes equations in a space-time domain, see for example [1, 2, 3],

$$\begin{aligned}
 (1a) \quad & \partial_t \mathbf{u} + \boldsymbol{\omega} \times \mathbf{u} + \text{Re}^{-1} \nabla \times \boldsymbol{\omega} + \nabla P = \mathbf{f} && \text{in } \Omega \times (0, T], \\
 (1b) \quad & \boldsymbol{\omega} - \nabla \times \mathbf{u} = \mathbf{0} && \text{in } \Omega \times (0, T], \\
 (1c) \quad & \nabla \cdot \mathbf{u} = 0 && \text{in } \Omega \times (0, T],
 \end{aligned}$$

where $\Omega \subset \mathbb{R}^2$, is a simply connected, bounded domain with a Lipschitz boundary $\partial\Omega$, $\partial_t := \frac{\partial}{\partial t}$, \mathbf{u} is the velocity field, $\boldsymbol{\omega}$ is the vorticity field, $P := p + \frac{1}{2} \mathbf{u} \cdot \mathbf{u}$ is the total pressure (with p being the static pressure), \mathbf{f} is the external (body) force, and Re denotes the Reynolds number. (1) is supplemented with an initial condition,

$$(2) \quad \mathbf{u}^0 = \mathbf{u}(\mathbf{x}, t_0),$$

and two pairs of boundary conditions,

$$(3) \quad \begin{cases} \mathbf{u} \cdot \mathbf{n} = \hat{u}_\perp & \text{on } \Gamma_\perp \times (0, T] \\ P = \hat{P} & \text{on } \Gamma_{\hat{P}} \times (0, T] \end{cases}, \quad \begin{cases} \boldsymbol{\omega} = \hat{\boldsymbol{\omega}} & \text{on } \Gamma_{\hat{\boldsymbol{\omega}}} \times (0, T] \\ \mathbf{u} \times \mathbf{n} = \hat{u}_\parallel & \text{on } \Gamma_\parallel \times (0, T] \end{cases},$$

where \mathbf{n} is the unit outward norm vector. In each pair, the boundary sections are disjoint, and therefore the boundary conditions are not active at the same boundary section, i.e., $\Gamma_\perp \cap \Gamma_{\hat{P}} = \Gamma_{\hat{\boldsymbol{\omega}}} \cap \Gamma_\parallel = \emptyset$, and each pair is active over the whole boundary, $\Gamma_\perp \cup \Gamma_{\hat{P}} = \Gamma_{\hat{\boldsymbol{\omega}}} \cup \Gamma_\parallel = \partial\Omega$, also see [4, Table 1]. Note that,

*Corresponding author

Email addresses: zhangyi_aero@hotmail.com (Yi Zhang), a.palha@tudelft.nl (Artur Palha), m.i.gerritsma@tudelft.nl (Marc Gerritsma), yaoqhe@sysu.edu.cn (Qinghe Yao)

Preprint submitted to arXiv

when $\Gamma_{\hat{p}} = \emptyset$, there is a singular mode in the total pressure of (1); the total pressure is determined up to a constant.

The divergence free condition of velocity, (1c), implies mass conservation. For two-dimensional incompressible flows, integral quantities of interest include

$$\begin{aligned} \text{total kinetic energy (or simply energy)} \mathcal{K} &:= \frac{1}{2} \int_{\Omega} \mathbf{u} \cdot \mathbf{u} \, d\Omega, \\ \text{total enstrophy (or simply enstrophy)} \mathcal{E} &:= \frac{1}{2} \int_{\Omega} \boldsymbol{\omega} \cdot \boldsymbol{\omega} \, d\Omega, \\ \text{total palinstrophy (or simply palinstrophy)} \mathcal{P} &:= \frac{1}{2} \int_{\Omega} (\nabla \times \boldsymbol{\omega}) \cdot (\nabla \times \boldsymbol{\omega}) \, d\Omega. \end{aligned}$$

In the absence of the external force¹, i.e., $\mathbf{f} = \mathbf{0}$, and if there is no net flux of energy and enstrophy over the domain boundary, two-dimensional incompressible flows dissipate energy at a rate,

$$(4) \quad \partial_t \mathcal{K} = -2\text{Re}^{-1} \mathcal{E},$$

and, additionally dissipate enstrophy at a rate,

$$(5) \quad \partial_t \mathcal{E} = -2\text{Re}^{-1} \mathcal{P}.$$

Furthermore, if the two-dimensional incompressible flow is in the inviscid limit ($\text{Re} \rightarrow \infty$), namely, the flow is ideal, from (4) and (5), it conserves energy and enstrophy over time [5]. And the relation (1b) implies

$$(6) \quad \mathcal{W} := \int_{\Omega} \boldsymbol{\omega} \, d\Omega = \oint_{\partial\Omega} \mathbf{u} \times \mathbf{n} \, d\Gamma,$$

where \mathcal{W} is called the total vorticity. (6) shows that the total vorticity no matter whether the flow is ideal or not, is a conserved quantity over time provided $\oint_{\partial\Omega} \mathbf{u} \times \mathbf{n} \, d\Gamma$ is not time dependent.

The first scheme that is mass, energy, enstrophy and vorticity conserving (MEEVC) was proposed in [5] where two evolution equations for velocity and vorticity are employed. The two evolution equations are staggered in time such that information can be transferred between each other through a midpoint temporal discretization scheme. As a result, both equations are linearized and the unknowns are decoupled to separate time instant sequences, which significantly lowers the computational cost. A drawback of this scheme is that the inclusion of no-slip boundary conditions requires indirect approaches and the suggested approach destroys the vorticity conservation property [6]. An extensive literature study on structure-preserving methods is given in [5]. For a more recent discussion on structure-preserving methods for incompressible flows, we refer, for example, to [7].

In this work, we introduce a mixed high-order finite element discretization of two-dimensional incompressible Navier-Stokes equations that is also MEEVC, can incorporate general boundary condition but avoids the evolution equation for vorticity. The functional setting will be given in Section 2. In Section 3, properties of the formulation are analyzed, which is followed by the introduction of the temporal discretization in Section 4. Numerical tests are presented in Section 5. Finally, conclusions are drawn in Section 6.

2. The mixed weak formulation

2.1. A brief introduction to function spaces employed

The space of square integrable functions, is

$$L^2(\Omega) := \{f \mid \langle f, f \rangle_{\Omega} \leq +\infty\},$$

where $\langle \cdot, \cdot \rangle_{\Omega}$ denotes the L^2 -inner product (or simply inner product) over the domain Ω . In \mathbb{R}^2 , we will also use Sobolev spaces

$$H(\text{curl}; \Omega) := \left\{ \boldsymbol{\omega} \mid \boldsymbol{\omega} \in L^2(\Omega), \nabla \times \boldsymbol{\omega} \in [L^2(\Omega)]^2 \right\},$$

¹Or when the external force is conservative.

$$\begin{aligned}
H(\operatorname{div}; \Omega) &:= \left\{ \mathbf{u} \mid \mathbf{u} \in [L^2(\Omega)]^2, \nabla \cdot \mathbf{u} \in L^2(\Omega) \right\}, \\
H^1(\Omega) &:= \left\{ \phi \mid \phi \in L^2(\Omega), \nabla \phi \in [L^2(\Omega)]^2 \right\}, \\
H(\operatorname{rot}; \Omega) &:= \left\{ \boldsymbol{\sigma} \mid \boldsymbol{\sigma} \in [L^2(\Omega)]^2, \nabla \times \boldsymbol{\sigma} \in L^2(\Omega) \right\}.
\end{aligned}$$

They form de Rham complexes [8] in two dimensions written as

$$\begin{aligned}
\mathbb{R} &\hookrightarrow H(\operatorname{curl}; \Omega) \xrightarrow{\nabla \times} H(\operatorname{div}; \Omega) \xrightarrow{\nabla \cdot} L^2(\Omega) \rightarrow 0, \\
\mathbb{R} &\hookrightarrow H^1(\Omega) \xrightarrow{\nabla} H(\operatorname{rot}; \Omega) \xrightarrow{\nabla \times} L^2(\Omega) \rightarrow 0.
\end{aligned}$$

Also see (1) and (2) of [9].

The trace operator, denoted by \mathcal{T} , restricts a function to a boundary section, $\Gamma \subseteq \partial\Omega$. The trace operator acting on $\omega \in H(\operatorname{curl}; \Omega)$, $\phi \in H^1(\Omega)$, $\mathbf{u} \in H(\operatorname{div}; \Omega)$ and $\boldsymbol{\sigma} \in H(\operatorname{rot}; \Omega)$ is, respectively,

$$\begin{aligned}
\mathcal{T}\omega &= \omega|_{\Gamma}, \quad \mathcal{T}\phi = \phi|_{\Gamma}, \\
\mathcal{T}\mathbf{u} &= \mathbf{u} \cdot \mathbf{n}|_{\Gamma}, \quad \mathcal{T}\boldsymbol{\sigma} = \boldsymbol{\sigma} \times \mathbf{n}|_{\Gamma}.
\end{aligned}$$

The trace spaces are

$$\begin{aligned}
\mathcal{TH}(\operatorname{curl}; \Omega, \Gamma) &:= \{ \mathcal{T}\omega \mid \omega \in H(\operatorname{curl}; \Omega) \}, \\
H^{-1/2}(\Omega, \Gamma) &:= \{ \mathcal{T}\mathbf{u} \mid \mathbf{u} \in H(\operatorname{div}; \Omega) \}, \\
H^{1/2}(\Omega, \Gamma) &:= \{ \mathcal{T}\phi \mid \phi \in H^1(\Omega) \}, \\
\mathcal{TH}(\operatorname{rot}; \Omega, \Gamma) &:= \{ \mathcal{T}\boldsymbol{\sigma} \mid \boldsymbol{\sigma} \in H(\operatorname{rot}; \Omega) \}.
\end{aligned}$$

Not that $\mathcal{TH}(\operatorname{curl}; \Omega, \Gamma)$ and $\mathcal{TH}(\operatorname{rot}; \Omega, \Gamma)$, as well as $H^{-1/2}(\Omega, \Gamma)$ and $H^{1/2}(\Omega, \Gamma)$, are a pair of dual spaces. For a complete introduction on Sobolev spaces, we refer to [10].

We use notations $C(\Omega)$, $D(\Omega)$, $G(\Omega)$, $R(\Omega)$ and $S(\Omega)$ to express finite dimensional conforming function spaces which are subsets of Sobolev spaces, i.e.,

$$\begin{aligned}
C(\Omega) &\subset H(\operatorname{curl}; \Omega), \quad D(\Omega) \subset H(\operatorname{div}; \Omega), \quad S(\Omega) \subset L^2(\Omega), \\
G(\Omega) &\subset H^1(\Omega), \quad R(\Omega) \subset H(\operatorname{rot}; \Omega),
\end{aligned}$$

and form discrete de Rham complexes in two-dimensional space,

$$\begin{aligned}
(7) \quad \mathbb{R} &\hookrightarrow C(\Omega) \xrightarrow{\nabla \times} D(\Omega) \xrightarrow{\nabla \cdot} S(\Omega) \rightarrow 0, \\
\mathbb{R} &\hookrightarrow G(\Omega) \xrightarrow{\nabla} R(\Omega) \xrightarrow{\nabla \times} S(\Omega) \rightarrow 0.
\end{aligned}$$

The finite dimensional spaces $C(\Omega)$ and $D(\Omega)$ possess sufficient regularity such that

$$(8) \quad \omega_h \times \mathbf{u}_h \in [L^2(\Omega)]^2, \quad \forall (\omega_h, \mathbf{u}_h) \in C(\Omega) \times D(\Omega).$$

Trace spaces of finite dimensional spaces $C(\Omega, \Gamma)$ and $d(\Omega, \Gamma)$ on boundary section Γ are denoted by

$$\begin{aligned}
\mathcal{TC}(\Omega, \Gamma) &:= \{ \mathcal{T}\omega_h \mid \omega_h \in C(\Omega) \}, \\
\mathcal{TD}(\Omega, \Gamma) &:= \{ \mathcal{T}\mathbf{u}_h \mid \mathbf{u}_h \in D(\Omega) \}.
\end{aligned}$$

And we will also use following subspaces,

$$\begin{aligned}
C_0(\Omega, \Gamma) &:= \{ \omega_h \mid \omega_h \in C(\Omega), \mathcal{T}\omega_h = 0 \in \mathcal{TC}(\Omega, \Gamma) \}, \\
D_0(\Omega, \Gamma) &:= \{ \mathbf{u}_h \mid \mathbf{u}_h \in D(\Omega), \mathcal{N}\mathbf{u}_h = 0 \in \mathcal{ND}(\Omega, \Gamma) \}.
\end{aligned}$$

2.2. The formulation

We introduce a trilinear form

$$a(\rho_h, \boldsymbol{\vartheta}_h, \mathbf{e}_h) := \int_{\Omega} (\rho_h \times \boldsymbol{\vartheta}_h) \cdot \mathbf{e}_h \, d\Omega,$$

for $(\rho_h, \boldsymbol{\vartheta}_h, \mathbf{e}_h) \in C(\Omega) \times D(\Omega) \times D(\Omega)$. Because $\rho_h \times \boldsymbol{\vartheta}_h$ is pointwise perpendicular to $\boldsymbol{\vartheta}_h$, we know that

$$(9) \quad a(\rho_h, \boldsymbol{\vartheta}_h, \boldsymbol{\vartheta}_h) = 0.$$

A spatially discrete weak mixed formulation of (1) is written as following: Given $\mathbf{f} \in [L^2(\Omega)]^2$ and natural boundary conditions, $\widehat{P} \in H^{1/2}(\Omega, \Gamma_{\widehat{P}})$ and $\widehat{u}_{\parallel} \in \mathcal{TH}(\text{rot}; \Omega, \Gamma_{\parallel})$, seek $(\mathbf{u}_h, \omega_h, P_h) \in D(\Omega) \times C(\Omega) \times S(\Omega)$, such that, $\forall (\mathbf{v}_h, \xi_h, q_h) \in D_0(\Omega, \Gamma_{\perp}) \times C_0(\Omega, \Gamma_{\widehat{\omega}}) \times S(\Omega)$,

$$(10a) \quad \langle \partial_t \mathbf{u}_h, \mathbf{v}_h \rangle_{\Omega} + a(\omega_h, \mathbf{u}_h, \mathbf{v}_h) + \text{Re}^{-1} \langle \nabla \times \omega_h, \mathbf{v}_h \rangle_{\Omega} - \langle P_h, \nabla \cdot \mathbf{v}_h \rangle_{\Omega} = \langle \mathbf{f}, \mathbf{v}_h \rangle_{\Omega} - \left\langle \widehat{P} \Big| \mathcal{T} \mathbf{v}_h \right\rangle_{\Gamma_{\widehat{P}}},$$

$$(10b) \quad \langle \mathbf{u}_h, \nabla \times \xi_h \rangle_{\Omega} - \langle \omega_h, \xi_h \rangle_{\Omega} = \langle \widehat{u}_{\parallel} \Big| \mathcal{T} \xi_h \rangle_{\Gamma_{\parallel}},$$

$$(10c) \quad \langle \nabla \cdot \mathbf{u}_h, q_h \rangle_{\Omega} = 0,$$

subject to essential boundary conditions, $\mathcal{T} \mathbf{u}_h = \widehat{u}_{\perp} \in \mathcal{TD}(\Omega, \Gamma_{\perp})$ and $\mathcal{T} \omega_h = \widehat{\omega} \in \mathcal{TC}(\Omega, \Gamma_{\widehat{\omega}})$, and initial conditions $(\mathbf{u}_h^0, \omega_h^0) \in D(\Omega) \times C(\Omega)$. Note that we have used the notation $\langle \cdot | \cdot \rangle_{\Gamma}$ to indicate that it is a duality pairing between elements from a pair of dual spaces.

One can show that $(\mathbf{u}_h, \omega_h, P_h)$ in (10) weakly solves the incompressible Navier-Stokes equations (1), see the work of Boffi, Brezzi and Fortin [11]. A similar setup is proposed in the fluid part of a structure-preserving formulation for magnetohydrodynamics (MHD) problems, cf. (48) - (53) of [12].

3. Dissipation and conservation properties

In this section, we study dissipation and conservation properties of the formulation (10). The equivalence between (10) and the formulation used in the original MEEVC scheme, see (19) of [5], will also be shown. Thus, we will prove that the formulation (10) is also MEEVC. To this end, the analysis conducted here is under conditions that (i) the domain is periodic ($\partial\Omega = \emptyset$) and (ii) there is no external force as in [5].

3.1. Mass conservation

Pointwise mass conservation is obviously satisfied; \mathbf{u}_h is selected to be in $D(\Omega) \subset H(\text{div}; \Omega)$ and the relation (10c) strongly enforces $\nabla \cdot \mathbf{u}_h = 0$ everywhere in Ω . This is a consequence of the fact that $\nabla \cdot$ maps $D(\Omega)$ into $S(\Omega)$, see (7).

3.2. Energy dissipation and conservation

For the energy balance, if we replace \mathbf{v}_h in (10a) by $\mathbf{u}_h \in D(\Omega)$, we will obtain

$$(11) \quad \langle \partial_t \mathbf{u}_h, \mathbf{u}_h \rangle_{\Omega} + a(\omega_h, \mathbf{u}_h, \mathbf{u}_h) + \text{Re}^{-1} \langle \nabla \times \omega_h, \mathbf{u}_h \rangle_{\Omega} - \langle P_h, \nabla \cdot \mathbf{u}_h \rangle_{\Omega} = 0.$$

The second and fourth terms vanish because of (9) and the pointwise mass conservation, i.e., $\nabla \cdot \mathbf{u}_h = 0$, respectively. This leads to

$$\langle \partial_t \mathbf{u}_h, \mathbf{u}_h \rangle_{\Omega} + \text{Re}^{-1} \langle \nabla \times \omega_h, \mathbf{u}_h \rangle_{\Omega} = 0.$$

And from (10b), we know

$$\langle \mathbf{u}_h, \nabla \times \omega_h \rangle_{\Omega} = \langle \omega_h, \omega_h \rangle_{\Omega},$$

because $\omega_h \in C(\Omega)$. Combining these two relations gives a (semi-)discrete energy balance,

$$(12) \quad \partial_t \mathcal{K}_h = \langle \partial_t \mathbf{u}_h, \mathbf{u}_h \rangle_{\Omega} = -\text{Re}^{-1} \langle \omega_h, \omega_h \rangle_{\Omega} = -2\text{Re}^{-1} \mathcal{E}_h,$$

where $\mathcal{K}_h = \frac{1}{2} \langle \mathbf{u}_h, \mathbf{u}_h \rangle_{\Omega}$ and $\mathcal{E}_h = \frac{1}{2} \langle \omega_h, \omega_h \rangle_{\Omega}$ are the discrete (total kinetic) energy and (total) enstrophy, respectively. It is consistent with (4), the energy balance of the strong form. Thus, (12) clearly implies discrete energy conservation in the inviscid limit ($\text{Re} \rightarrow \infty$).

3.3. Enstrophy dissipation and conservation

If we take the time derivative of (10b), we obtain

$$(13) \quad \langle \partial_t \mathbf{u}_h, \nabla \times \xi_h \rangle_\Omega = \langle \partial_t \omega_h, \xi_h \rangle_\Omega, \quad \forall \xi_h \in C(\Omega).$$

And, from (10a), we know that, $\forall \xi_h \in C(\Omega)$, (10a) must hold for $\nabla \times \xi_h \in D(\Omega)$, namely,

$$(14) \quad \langle \partial_t \mathbf{u}_h, \nabla \times \xi_h \rangle_\Omega + a(\omega_h, \mathbf{u}_h, \nabla \times \xi_h) + \text{Re}^{-1} \langle \nabla \times \omega_h, \nabla \times \xi_h \rangle_\Omega - \langle P_h, \nabla \cdot \nabla \times \xi_h \rangle_\Omega = 0,$$

where the term $\langle P_h, \nabla \cdot \nabla \times \xi_h \rangle_\Omega$ vanishes because $\nabla \cdot \nabla \times (\cdot) \equiv 0$. If we further insert (13) into (14), we obtain

$$(15) \quad \langle \partial_t \omega_h, \xi_h \rangle_\Omega + a(\omega_h, \mathbf{u}_h, \nabla \times \xi_h) + \text{Re}^{-1} \langle \nabla \times \omega_h, \nabla \times \xi_h \rangle_\Omega = 0, \quad \forall \xi_h \in C(\Omega).$$

We can replace ξ_h in (15) by $\omega_h \in C(\Omega)$ and get

$$(16) \quad \langle \partial_t \omega_h, \omega_h \rangle_\Omega + a(\omega_h, \mathbf{u}_h, \nabla \times \omega_h) + \text{Re}^{-1} \langle \nabla \times \omega_h, \nabla \times \omega_h \rangle_\Omega = 0.$$

As $\mathbf{u}_h \in D(\Omega)$ and $\nabla \cdot \mathbf{u}_h = 0$ is satisfied pointwise, we can find a stream function $\psi_h \in C(\Omega)$ (on the simply connected, contractible domain) such that $\mathbf{u}_h = \nabla \times \psi_h$. Recall the following vector calculus identity,

$$\omega_h \times \nabla \times \psi_h = \nabla(\omega_h \psi_h) - \psi_h \times \nabla \times \omega_h.$$

Thus we know

$$\begin{aligned} a(\omega_h, \mathbf{u}_h, \nabla \times \omega_h) &= \int_\Omega \nabla(\omega_h \psi_h) \cdot (\nabla \times \omega_h) \, d\Omega - a(\psi_h, \nabla \times \omega_h, \nabla \times \omega_h) \\ &= \int_\Omega \omega_h \psi_h (\nabla \cdot \nabla \times \omega_h) \, d\Omega - a(\psi_h, \nabla \times \omega_h, \nabla \times \omega_h), \end{aligned}$$

where we have performed integration by parts with respect to the gradient operator for the first term of the second equality and use the periodic boundary condition. Obviously, these terms vanish because of property $\nabla \cdot \nabla \times (\cdot) \equiv 0$ and (9). Therefore, we know that

$$(17) \quad a(\omega_h, \mathbf{u}_h, \nabla \times \omega_h) = 0,$$

and (16) leads to the following (semi-)discrete enstrophy balance,

$$(18) \quad \langle \partial_t \omega_h, \omega_h \rangle_\Omega = -\text{Re}^{-1} \langle \nabla \times \omega_h, \nabla \times \omega_h \rangle_\Omega = -2\text{Re}^{-1} \mathcal{P}_h,$$

where $\mathcal{P}_h := \frac{1}{2} \langle \nabla \times \omega_h, \nabla \times \omega_h \rangle_\Omega$ is the discrete (total) palinstrophy. (18) correctly reflects the enstrophy balance of the strong form, see (5). And, in the inviscid limit ($\text{Re} \rightarrow \infty$), (18) leads to enstrophy conservation.

3.4. Vorticity conservation

For conservation of (total) vorticity, if we select $\xi_h = 1$ in (14), it is straightforward to find that

$$\partial_t \mathcal{W}_h = \langle \partial_t \omega_h, 1 \rangle_\Omega = 0,$$

which implies that vorticity is conserved over time. Moreover, by selecting $\xi_h = 1$ in (10b), we know that in periodic domains

$$\mathcal{W}_h \equiv 0,$$

which is consistent with (6) of the strong form.

3.5. Equivalence to the original MEEVC formulation

If we apply integration by parts to the second term of (15), we obtain

$$(19) \quad \langle \partial_t \omega_h, \xi_h \rangle_\Omega + \langle \nabla \times (\omega_h \times \mathbf{u}_h), \xi_h \rangle_h + \text{Re}^{-1} \langle \nabla \times \omega_h, \nabla \times \xi_h \rangle_\Omega = 0.$$

Recall that the following identity

$$(20) \quad \nabla \times (\omega_h \times \mathbf{u}_h) = \frac{1}{2} (\mathbf{u}_h \cdot \nabla) \omega_h + \frac{1}{2} \nabla \cdot (\omega_h \mathbf{u}_h),$$

is valid in two-dimensions. Using this identity, the following substitution can be employed in the weak form of the vorticity evolution equation (19),

$$(21) \quad \begin{aligned} \langle \nabla \times (\omega_h \times \mathbf{u}_h), \xi_h \rangle_\Omega &= \frac{1}{2} \langle (\mathbf{u}_h \cdot \nabla) \omega_h, \xi_h \rangle_\Omega + \frac{1}{2} \langle \nabla \cdot (\omega_h \mathbf{u}_h), \xi_h \rangle_\Omega \\ &= -\frac{1}{2} \langle \omega_h, \nabla \cdot (\xi_h \mathbf{u}_h) \rangle_\Omega + \frac{1}{2} \langle \nabla \cdot (\omega_h \mathbf{u}_h), \xi_h \rangle_\Omega, \end{aligned}$$

where the following integration by parts was used,

$$\langle (\mathbf{u}_h \cdot \nabla) \omega_h, \xi_h \rangle_\Omega = -\langle \omega_h, \nabla \cdot (\xi_h \mathbf{u}_h) \rangle_\Omega.$$

Thus, $\forall \xi_h \in C(\Omega)$, (19) can be written as

$$(22) \quad \langle \partial_t \omega_h, \xi_h \rangle_\Omega - \frac{1}{2} \langle \omega_h, \nabla \cdot (\xi_h \mathbf{u}_h) \rangle_\Omega + \frac{1}{2} \langle \nabla \cdot (\omega_h \mathbf{u}_h), \xi_h \rangle_\Omega + \text{Re}^{-1} \langle \nabla \times \omega_h, \nabla \times \xi_h \rangle_\Omega = 0,$$

which is the weak evolution equation for vorticity (as a replacement of (10b)) in the original MEEVC scheme, see (19) of [5]. If we select ξ_h to be ω_h in (22), the second and third terms cancel, we again get the same enstrophy balance, i.e., (18).

In the original MEEVC work, the reason behind using the identity (20) is to replace the weak nonlinear advection term by (21). By doing so, it is possible to construct another trilinear form for the nonlinear advection term in the weak vorticity evolution equation which is skew-symmetric with respect to entries ω_h and ξ_h , i.e.,

$$b(\omega_h, \mathbf{u}_h, \xi_h) = -b(\xi_h, \mathbf{u}_h, \omega_h).$$

See second and third terms in (22). This then implies that

$$b(\omega_h, \mathbf{u}_h, \omega_h) = 0,$$

which, for the original MEEVC work, is a key requirement to obtain enstrophy conservation even when the numerical quadrature is inexact. However, this prevents the direct incorporation of boundary conditions for the tangential component of velocity because the part, i.e., the boundary integral term in (10b) which is used to impose them weakly, is missing. In this present work, we surprisingly find that, to setup a MEEVC scheme, we can bypass the construction of the skew-symmetric advection term as in the original MEEVC scheme and, thus, it is not necessary to introduce a second evolution equation for vorticity. This simplifies the formulation and also enables the direct application of no-slip boundary conditions.

4. Temporal discretization

For the temporal discretization, the classic implicit midpoint method [13] is used. The fully discrete version of (10) is written as: Given $\mathbf{f} \in [L^2(\Omega)]^2$ and natural boundary conditions, $\widehat{P} \in H^{1/2}(\Omega, \Gamma_{\widehat{P}})$ and $\widehat{u}_\parallel \in \mathcal{TH}(\text{rot}; \Omega, \Gamma_\parallel)$, for $k \in \{1, 2, 3, \dots\}$, seek $(\mathbf{u}_h^k, \omega_h^k, P_h^{k-\frac{1}{2}}) \in D(\Omega) \times C(\Omega) \times S(\Omega)$, such that, $\forall (\mathbf{v}_h, \xi_h, q_h) \in D_0(\Omega, \Gamma_\perp) \times C_0(\Omega, \Gamma_{\widehat{P}}) \times S(\Omega)$,

$$(23a) \quad \left\langle \frac{\mathbf{u}_h^k - \mathbf{u}_h^{k-1}}{\Delta t}, \mathbf{v}_h \right\rangle_\Omega + a \left(\frac{\omega_h^{k-1} + \omega_h^k}{2}, \frac{\mathbf{u}_h^{k-1} + \mathbf{u}_h^k}{2}, \mathbf{v}_h \right) + \text{Re}^{-1} \left\langle \nabla \times \frac{\omega_h^{k-1} + \omega_h^k}{2}, \mathbf{v}_h \right\rangle_\Omega \\ - \left\langle P_h^{k-\frac{1}{2}}, \nabla \cdot \mathbf{v}_h \right\rangle_\Omega = \left\langle \mathbf{f}^{k-\frac{1}{2}}, \mathbf{v}_h \right\rangle_\Omega - \left\langle \widehat{P}^{k-\frac{1}{2}} \Big| \mathcal{T} \mathbf{v}_h \right\rangle_{\Gamma_{\widehat{P}}},$$

$$(23b) \quad \langle \mathbf{u}_h^k, \nabla \times \xi_h \rangle_\Omega - \langle \omega_h^k, \xi_h \rangle_\Omega = \left\langle \widehat{u}_\parallel^k \Big| \mathcal{T} \xi_h \right\rangle_{\Gamma_\parallel},$$

$$(23c) \quad \langle \nabla \cdot \mathbf{u}_h^k, q_h \rangle_\Omega = 0,$$

where $\Delta t = t_k - t_{k-1} > 0$, $\mathbf{u}_h^k = \mathbf{u}_h(\mathbf{x}, t_k)$ (see (2)), subject to essential boundary conditions, $\mathcal{T}\mathbf{u}_h^k = \widehat{\mathbf{u}}_\perp \in \mathcal{TD}(\Omega, \Gamma_\perp)$ and $\mathcal{T}\omega_h^k = \widehat{\omega} \in \mathcal{TC}(\Omega, \Gamma_{\widehat{\omega}})$, and initial conditions $(\mathbf{u}_h^0, \omega_h^0) \in D(\Omega) \times C(\Omega)$.

At the fully discrete level, if we repeat the analysis in Section 3 now for the fully discrete formulation (23), we can find that pointwise conservation of mass is satisfied at each time instant, see (23c), i.e.,

$$\nabla \cdot \mathbf{u}_h^k = 0$$

everywhere in Ω . And we can also obtain dissipation rates,

$$(24) \quad \frac{\mathcal{K}_h^k - \mathcal{K}_h^{k-1}}{\Delta t} = \left\langle \frac{\mathbf{u}_h^k - \mathbf{u}_h^{k-1}}{\Delta t}, \frac{\mathbf{u}_h^{k-1} + \mathbf{u}_h^k}{2} \right\rangle_\Omega = -\text{Re}^{-1} \left\langle \omega_h^{k-\frac{1}{2}}, \omega_h^{k-\frac{1}{2}} \right\rangle_\Omega = -2\text{Re}^{-1} \mathcal{E}_h^{k-\frac{1}{2}},$$

$$(25) \quad \frac{\mathcal{E}_h^k - \mathcal{E}_h^{k-1}}{\Delta t} = \left\langle \frac{\omega_h^k - \omega_h^{k-1}}{\Delta t}, \frac{\omega_h^{k-1} + \omega_h^k}{2} \right\rangle_\Omega = -\text{Re}^{-1} \left\langle \nabla \times \omega_h^{k-\frac{1}{2}}, \nabla \times \omega_h^{k-\frac{1}{2}} \right\rangle_\Omega = -2\text{Re}^{-1} \mathcal{P}_h^{k-\frac{1}{2}},$$

and

$$\frac{\mathcal{W}_h^k - \mathcal{W}_h^{k-1}}{\Delta t} = \left\langle \frac{\omega_h^k - \omega_h^{k-1}}{\Delta t}, 1 \right\rangle_\Omega = 0,$$

where $\omega_h^{k-\frac{1}{2}} := \frac{\omega_h^{k-1} + \omega_h^k}{2}$. This shows that at the fully discrete level the proposed scheme is also MEEVC in the inviscid limit, $\text{Re} \rightarrow \infty$.

5. Numerical tests

Four tests are conducted in this work. The accuracy of the method is investigated with an analytical solution in Section 5.1. Conservation and dissipation properties are tested in Section 5.2. The original MEEVC scheme experiences difficulties of handling no-slip boundary conditions [6] while imposing different boundary conditions including the no-slip ones is straightforward for the method studied in this work. This is demonstrated in Section 5.3. Numerical evidences of (17) is given by the test in Section 5.4.

We use the mimetic polynomial spaces, which satisfy the discrete de Rham complex (7) and the regularity (8), as the finite dimensional spaces under the framework of the mimetic spectral element method, see, for example, [14] or [15, Chapter 2]. The degree of the polynomial spaces is denoted by N . The Newton-Raphson method is employed for solving the nonlinear systems. Both orthogonal and curvilinear meshes will be used. Suppose a reference domain is $\hat{\Omega} := (r, s) \in [0, 1]^2$. A uniform orthogonal mesh of $K \times K$ square elements is generated in the reference domain. This mesh is then distorted with a mapping, $\Phi : (r, s) \rightarrow (x, y)$, expressed as

$$(26) \quad \begin{cases} x = \alpha \left(r + \frac{1}{2} c \sin(2\pi r) \sin(2\pi s) \right) \\ y = \alpha \left(s + \frac{1}{2} c \sin(2\pi r) \sin(2\pi s) \right) \end{cases},$$

where $\alpha > 0$ and $0 \leq c \leq 0.3$. It gives a mesh in $\Omega = (x, y) \in [0, \alpha]^2$, and the factor c is a deformation factor. When $c = 0$ the mesh is orthogonal and uniform, and when $c > 0$ the mesh is curvilinear. See Fig. 1 for illustrations of this mesh. And see [16] for an introduction on mesh deformation.

Implementations of the present work are done in *Python*.

5.1. Accuracy test: Taylor–Green vortex

We test the accuracy of the method using a classic analytical solution of two-dimensional incompressible Navier-Stokes equations in the absence of external force, the Taylor–Green vortex, written as

$$\begin{aligned} u(x, y, t) &= -\sin(\pi x) \cos(\pi y) e^{-2\pi^2 t/\text{Re}}, \\ v(x, y, t) &= \cos(\pi x) \sin(\pi y) e^{-2\pi^2 t/\text{Re}}, \\ p(x, y, t) &= \frac{1}{4} (\cos(2\pi x) + \cos(2\pi y)) e^{-4\pi^2 t/\text{Re}}, \\ \omega(x, y, t) &= -2\pi \sin(\pi x) \sin(\pi y) e^{-2\pi^2 t/\text{Re}}. \end{aligned}$$

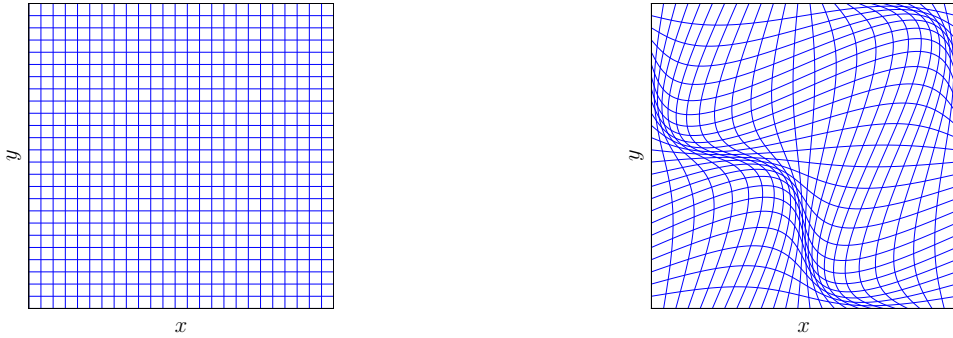


Figure 1: Illustrations of meshes implied by (26) for $K = 25$, deformation factor $c = 0$ (left) and $c = 0.25$ (right).

The domain is set to $\Omega = (x, y) \in [0, 2]^2$ with periodic boundary conditions. We use the meshes described by (26) and solve the Taylor–Green vortex from $t = t_0 = 0$ to $t = 1$ with $\text{Re} = 100$ and $\Delta t = \frac{1}{25}$. Results showing optimal convergence rates are presented in Fig. 2.

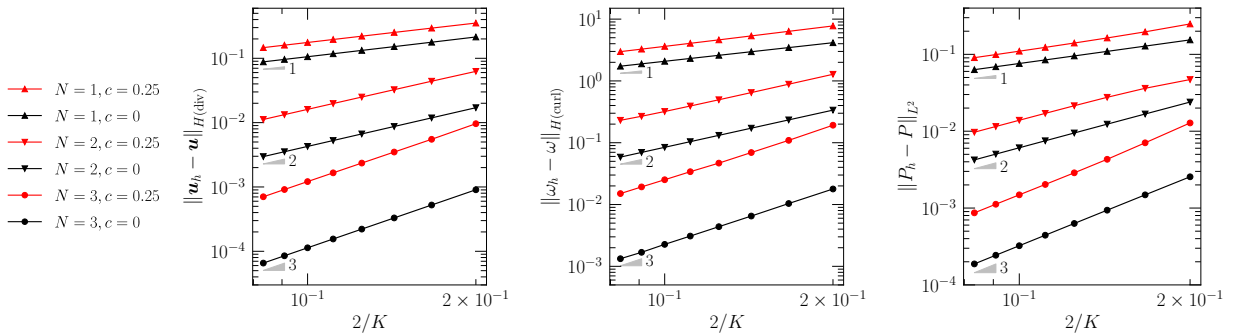


Figure 2: $H(\text{div})$ -error of \mathbf{u}_h , $H(\text{curl})$ -error of ω_h and L^2 -error of P_h at $t = 1$ of the Taylor–Green vortex test under ph -refinements for $N \in \{1, 2, 3\}$, $c \in \{0, 0.25\}$, $K \in \{10, 12, 14 \dots, 24\}$, $\Delta t = \frac{1}{25}$ and $\text{Re} = 100$.

5.2. Conservation and dissipation tests: Shear layer roll-up

The shear layer roll-up is a two-dimensional ideal flow whose initial condition is given by

$$u^0 = \begin{cases} \tanh\left(\frac{y - \pi/2}{\delta}\right), & y \leq \pi \\ \tanh\left(\frac{3\pi/2 - y}{\delta}\right), & y > \pi \end{cases}, \quad v^0 = \epsilon \sin(x),$$

where $\delta = \frac{\pi}{15}$ and $\epsilon = 0.05$, see [5, 17]. The domain is $\Omega = (x, y) \in [0, 2\pi]^2$ with periodic boundary conditions. Meshes as described in (26) for $c \in \{0, 0.25\}$ and $K = 48$ are used. The polynomial degree is set to $N = 2$ and the time interval is $\Delta t = \frac{1}{50}$. The flow is computed from $t = t_0 = 0$ to $t = 8$. To limit the error caused by the Newton-Raphson method, the tolerance of outer iterations is set to 10^{-12} . The vorticity field ω_h at $t \in \{0, 4, 8\}$ for $c = 0$ is shown in Fig. 3. In Fig. 4, results showing the conservation laws are satisfied to machine precision on both orthogonal and curvilinear meshes are presented. And throughout this section we use $\|\nabla \cdot \mathbf{u}_h\|_{L^2}$, i.e. the L^2 -norm of $\nabla \cdot \mathbf{u}_h$, to identify mass conservation. Since the basis functions have normal continuity, if $\|\nabla \cdot \mathbf{u}_h\|_{L^2} = 0$ (to machine precision), pointwise mass conservation is satisfied everywhere.

We repeat the above test now for a viscous flow of $\text{Re} = 500$. The results are presented in Fig. 5. It is seen that, to machine precision, (i) mass and vorticity conservation and (ii) energy and enstrophy balances, (24) and (25), are satisfied for both orthogonal and curvilinear meshes.

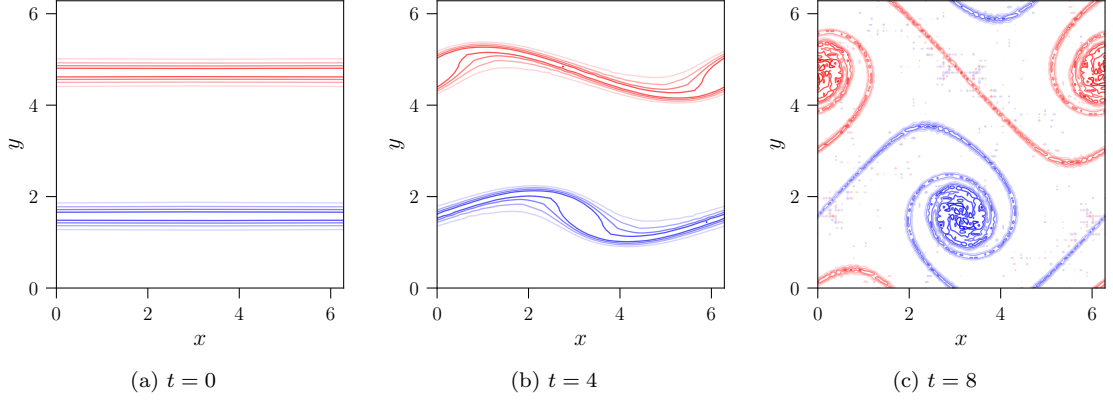


Figure 3: Vorticity field ω_h of the ideal shear layer roll-up test at $t \in \{0, 4, 8\}$ with contour lines for $\omega_h \in \{\pm 1, \pm 2, \pm 3, \dots, \pm 6\}$. The color scheme is from blue ($-6 \leftarrow \omega_h$) to red ($\omega_h \rightarrow 6$). The simulation is conducted for $N = 2$, $c = 0$, $K = 48$, $\Delta t = \frac{1}{50}$.

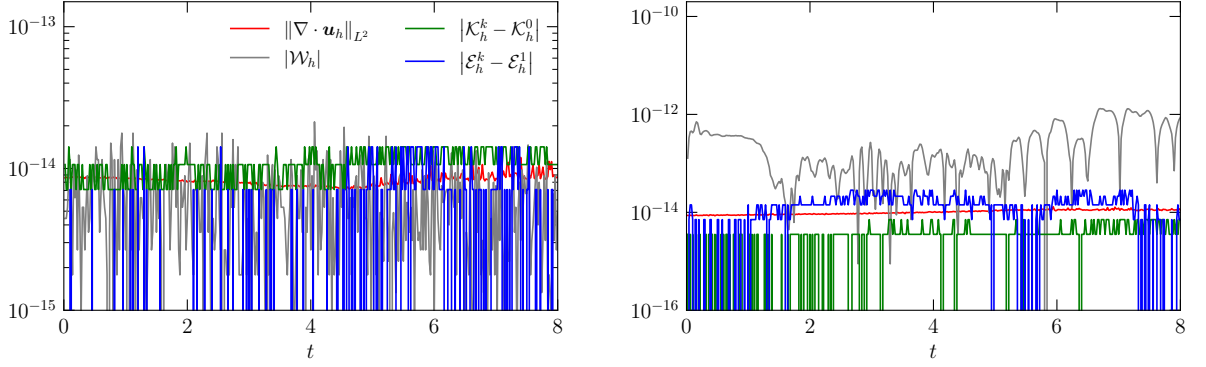


Figure 4: Discrete mass, energy, enstrophy and vorticity conservation over time of the ideal shear layer roll-up test for $N = 2$, $c = 0$ (left), $c = 0.25$ (right), $K = 48$ and $\Delta t = \frac{1}{50}$.

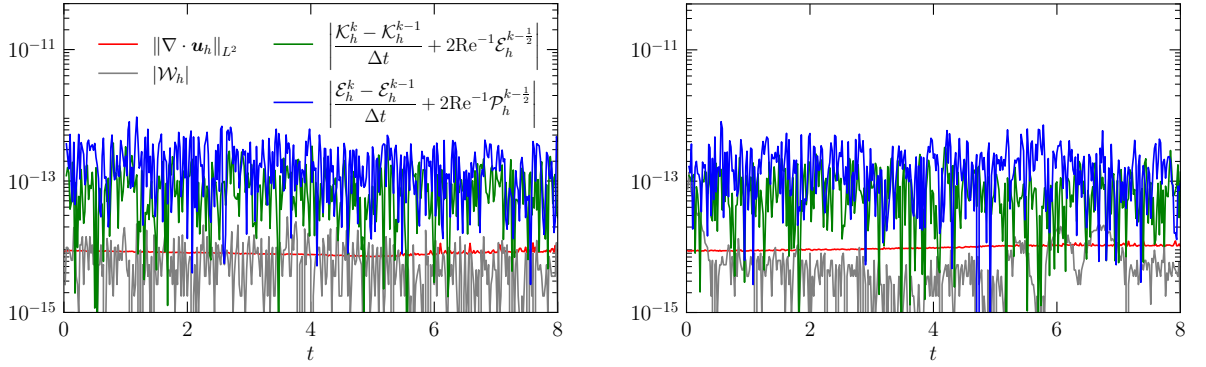


Figure 5: Discrete mass conservation, energy and enstrophy balances, and vorticity conservation over time of the viscous shear layer roll-up test for $N = 2$, $c = 0$ (left), $c = 0.25$ (right), $K = 48$, $\Delta t = \frac{1}{50}$ and $\text{Re} = 500$.

5.3. No-slip boundary condition test: Normal dipole collision

The normal dipole collision is a viscous flow in the domain $\Omega = (x, y) \in [-1, 1]^2$ with no-slip boundary conditions on all four walls [18]. The unscaled initial velocity field, $\mathbf{u}^0 = [u^0 \ v^0]$, is given by

$$\begin{aligned} u^0 &= -\frac{1}{2} |\omega_e| (y - y_1) e^{-(r_1/r_0)^2} + \frac{1}{2} |\omega_e| (y - y_2) e^{-(r_2/r_0)^2}, \\ v^0 &= -\frac{1}{2} |\omega_e| (x - x_2) e^{-(r_2/r_0)^2} + \frac{1}{2} |\omega_e| (x - x_1) e^{-(r_1/r_0)^2}, \end{aligned}$$

where $|\omega_e| = 320$, $(x_1, y_1) = (0, 0.1)$ and $(x_2, y_2) = (0, -0.1)$, r_1 and r_2 are distances to (x_1, y_1) and (x_2, y_2) , respectively, and $r_0 = 0.1$. This velocity field leads to a vorticity field expressed as

$$\omega^0 = \sum_{i \in \{1,2\}} \omega_{e,i} \left(1 - \left(\frac{r_i}{r_0} \right)^2 \right) e^{-(r_i/r_0)^2},$$

where $\omega_{e,1} = 320$, $\omega_{e,2} = -320$, which is a combination of two monopoles centered at (x_1, y_1) and (x_2, y_2) , respectively. The initial velocity is then scaled such that the initial kinetic energy is $\mathcal{E}^0 = 2$. The scaling factor is $f \approx 0.936026$. The corresponding initial enstrophy and palinstrophy are $\mathcal{E}^0 \approx 800$ and $\mathcal{P}^0 \approx 441855$, respectively. For the present test, we use a non-uniform orthogonal mesh of 5148 elements, see Fig. 6, $\text{Re} = 625$, polynomial degree $N = 2$ and $\Delta t = \frac{1}{200}$. This setup is similar to that in [6] except that [6] uses an unstructured mesh and much smaller time steps, $\Delta t = \frac{1}{2000}$.

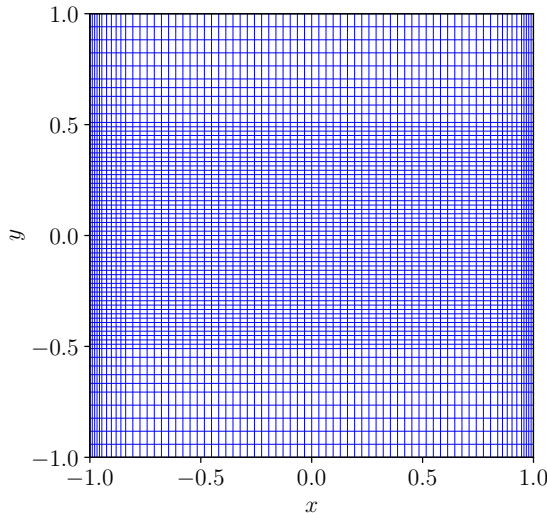


Figure 6: The mesh of 5148 elements used in the normal dipole collision test.

The dipole is initialized at $t = t_0 = 0$. It will move under a self-induced velocity in positive x -direction with an induced wake moving in the opposite direction. The simulation is performed until $t = 1$. The vorticity field ω_h at $t \in \{0, \frac{1}{5}, \frac{2}{5}, \dots, 1\}$ is presented in Fig. 7.

The original MEEVC scheme uses indirect approaches to impose no-slip boundary conditions, and the suggested approach, called the kinematic Neumann approach, destroys vorticity conservation, see [6, Fig. 9]. In contrast, the present method can handle no-slip boundary conditions (and other general boundary conditions) naturally, see the formulation (10) or (23). In Fig. 8, local distributions of vorticity field in region $(x, y) \in [0.4, 1] \times [-0.6, 0]$ at $t = 1$ and on boundary section $(x, y) \in -1 \times [-0.6, 0]$ at different time instants (with comparisons to results in [18]) are shown. The discrete energy, enstrophy and palinstrophy over time are presented and compared to results taken from [6, 18] in Fig. 9 where mass and vorticity conservation is also shown. These results show an improved match with the reference than those in [6, Fig. 10] and also indicate that no-slip boundary conditions are correctly incorporated by the present method without destroying vorticity conservation.

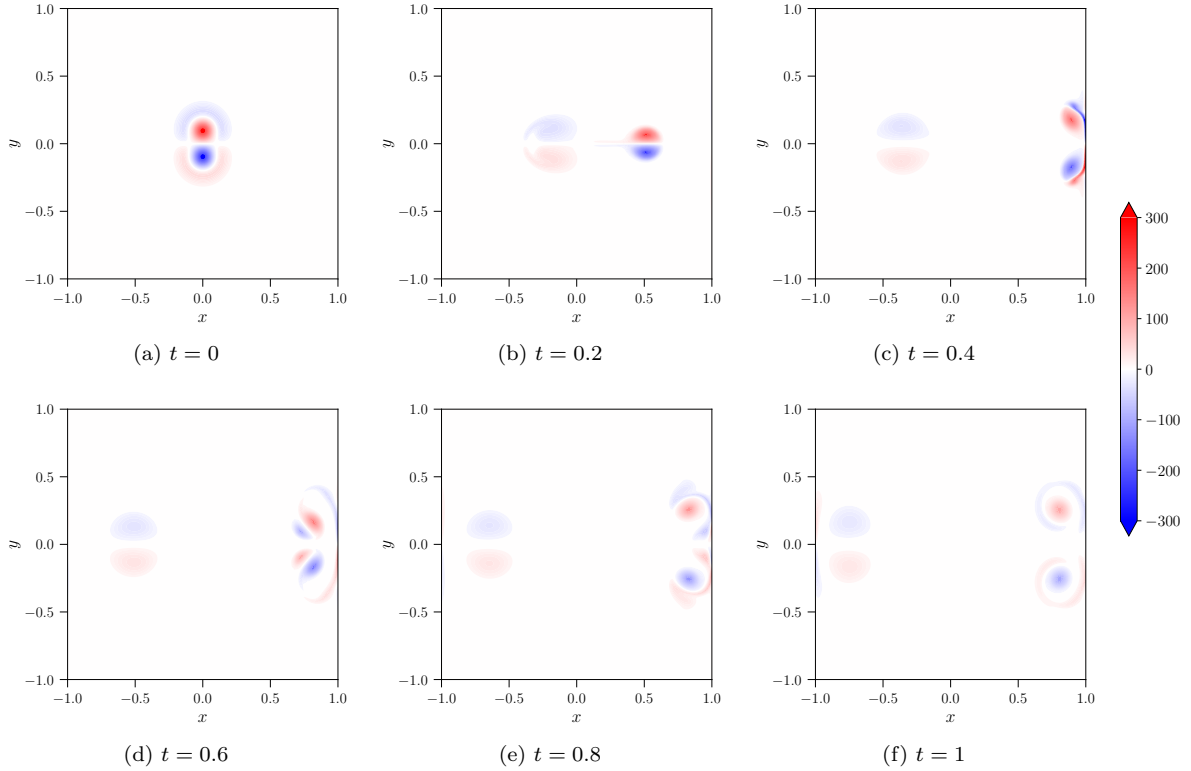


Figure 7: Vorticity field ω_h at $t \in \{0, \frac{1}{5}, \frac{2}{5}, \dots, 1\}$ of the normal dipole collision test in a mesh of 5148 elements for $N = 2$, $\Delta t = \frac{1}{200}$ and $\text{Re} = 625$.

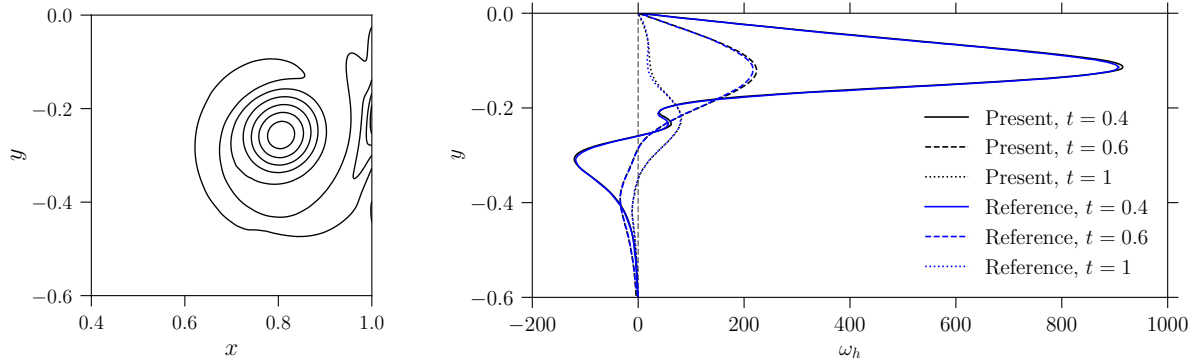


Figure 8: Vorticity field ω_h in region $(x, y) \in [0.4, 1] \times [-0.6, 0]$ at $t = 1$ with contour lines for $\omega_h \in \{-90, -70, -50, \dots, 70\}$ and on the boundary section $(x, y) \in -1 \times [-0.6, 0]$ at $t \in \{0.4, 0.6, 1\}$ compared to reference results taken from [18, Fig. 5] for $\text{Re} = 625$. The present simulation has 145^2 degrees of freedom for vorticity. The reference simulation uses a pseudospectral method and has 256^2 degrees of freedom for vorticity.

5.4. Convective term for enstrophy conservation

This subsection provides numerical evidences for (17) as it is a key for the enstrophy balance of the present method. Given two random smooth scalar fields,

$$\omega = 2\pi \sin(2\pi x + e) \sin(2\pi y + f)$$

and

$$\psi = 2\pi \sin(2\pi x + g) \sin(2\pi y + h),$$

where $e, f, g, h \in (0, 1)$ are random real numbers, in the periodic unit square, $\Omega = (x, y) \in [0, 1]^2$. In this domain, meshes as described in (26) for $c \in \{0, 0.25\}$ and $K = 12$ are generated. ω and ψ are projected

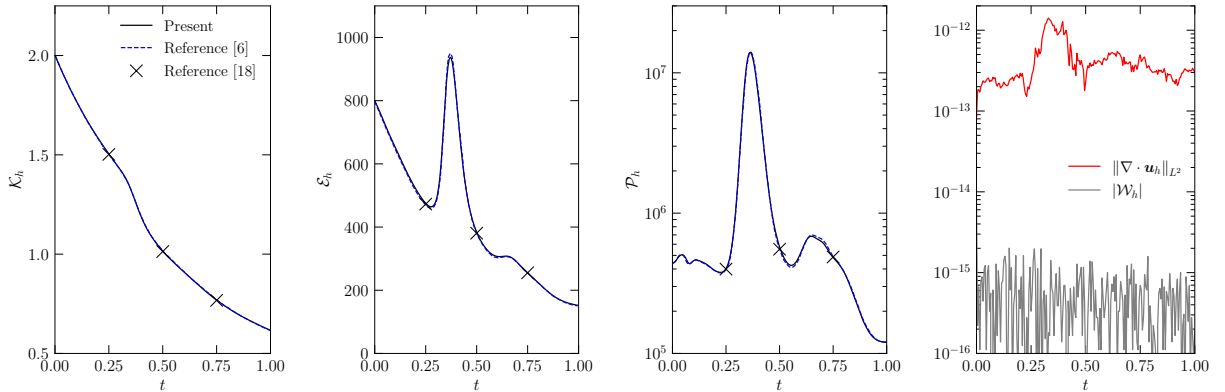


Figure 9: Discrete energy, enstrophy, palinstrophy over time compared to reference results taken from [6, Fig. 8] and reference results at $t \in \{0.25, 0.5, 0.75\}$ taken from [18], and mass and vorticity conservation over time.

to finite dimensional polynomial spaces as ω_h and ψ_h , see [14] or [15] for details of these projections. The finite dimensional velocity is $\mathbf{u}_h = \nabla \times \psi_h$ and thus $\nabla \cdot \mathbf{u}_h = 0$. Then the trilinear form $a(\omega_h, \mathbf{u}_h, \nabla \times \omega_h)$ is computed with Gauss quadrature, see [19], of different degrees, N_Q .

The results are presented in Table 1. We can see that, for the orthogonal mesh ($c = 0$), the trilinear form is zero (to machine precision) even when the quadrature is very inexact, for example, $N = 4$ and $N_Q = 1$ (numerical quadrature of degree N_Q is exact for polynomials of degree $N \leq 2N_Q - 1$). While for the curvilinear mesh ($c = 0.25$), as the metric of the mapping, see (26), cannot be captured by polynomials, the quadrature is always inexact and the trilinear form is still zero for quadrature degree that is significantly high. These results support the statement that, for $\nabla \cdot \mathbf{u}_h = 0$, the trilinear form $a(\omega_h, \mathbf{u}_h, \nabla \times \omega_h)$ can be zero even with inexact numerical quadrature.

Table 1: $a(\omega_h, \mathbf{u}_h, \nabla \times \omega_h)$ for $c \in \{0, 0.25\}$, $K = 12$, $N \in \{2, 3, 4\}$ and $N_Q \in \{1, 2, 3, 4, 5, 6\}$.

N_Q	c N	0			0.25		
		2	3	4	2	3	4
1		$1.05e - 12$	$4.72e - 12$	$-7.59e - 11$	$-1.91e + 02$	$-6.93e + 00$	$1.25e + 01$
2		$-1.60e - 12$	$2.25e - 12$	$1.04e - 12$	$-5.19e - 12$	$7.43e + 00$	$3.22e - 01$
3		$2.81e - 13$	$-1.01e - 12$	$3.65e - 14$	$6.51e - 12$	$1.55e - 03$	$-7.90e - 02$
4		$1.65e - 12$	$7.96e - 13$	$1.01e - 13$	$-7.46e - 14$	$-9.95e - 14$	$-1.48e - 04$
5		$-5.22e - 12$	$1.86e - 12$	$-7.21e - 14$	$1.70e - 12$	$5.68e - 13$	$-1.42e - 13$
6		$3.46e - 14$	$5.59e - 15$	$1.71e - 13$	$1.19e - 13$	$-2.52e - 13$	$2.23e - 13$

6. Conclusions

In this work, we present a mass, energy, enstrophy and vorticity conserving (MEEVC) mixed finite element discretization for the rotational form of the incompressible Navier-Stokes equations on both orthogonal and curvilinear meshes. Comparing to the original MEEVC method, the present method uses a formulation of a single evolution equation and, more importantly, can naturally adapt no-slip boundary conditions without damaging vorticity conservation. However, it does not linearize the discrete systems as the original MEEVC scheme does; a more expensive nonlinear method has to be employed to solve the systems.

Acknowledgements

The authors acknowledge dr. Andrea Brugnoli for helpful discussions.

References

- [1] T. A. Zang, On the rotation and skew-symmetric forms for incompressible flow simulations, *Applied Numerical Mathematics* 7 (1) (1991) 27–40.
- [2] W. Layton, C. C. Manica, M. Neda, M. Olshanskii, L. G. Rebholz, On the accuracy of the rotation form in simulations of the Navier–Stokes equations, *Journal of Computational Physics* 228 (9) (2009) 3433–3447.
- [3] X. Zhang, D. Schmidt, B. Perot, Accuracy and conservation properties of a three-dimensional unstructured staggered mesh scheme for fluid dynamics, *Journal of Computational Physics* 175 (2) (2002) 764–791. doi:<https://doi.org/10.1006/jcph.2001.6973>.
- [4] J. Kreeft, M. Gerritsma, Mixed mimetic spectral element method for Stokes flow: A pointwise divergence-free solution, *Journal of Computational Physics* 240 (2013) 284–309.
- [5] A. Palha, M. Gerritsma, A mass, energy, enstrophy and vorticity conserving (MEEVC) mimetic spectral element discretization for the 2D incompressible Navier-Stokes equations, *Journal of Computational Physics* 328 (2017) 200–220.
- [6] G. de Diego, A. Palha, M. Gerritsma, Inclusion of no-slip boundary conditions in the MEEVC scheme, *Journal of Computational Physics* 378 (2019) 615–633.
- [7] E. S. Gawlik, F. Gay-Balmaz, A conservative finite element method for the incompressible Euler equations with variable density, *Journal of Computational Physics* 412 (2020) 109439. doi:<https://doi.org/10.1016/j.jcp.2020.109439>.
- [8] P. B. Bochev, J. M. Hyman, Principles of mimetic discretizations of differential operators, in: *Compatible Spatial Discretizations*, Springer New York, 2006, pp. 89–119.
- [9] S. H. Christiansen, J. Hu, K. Hu, Nodal finite element de Rham complexes, *Numerische Mathematik* 139 (2) (2018) 411–446.
- [10] J. T. Oden, L. F. Demkowicz, *Applied Functional Analysis*, Second Edition, Taylor & Francis, 2010.
- [11] D. Boffi, F. Brezzi, M. Fortin, et al., *Mixed finite element methods and applications*, Vol. 44, Springer, 2013.
- [12] E. S. Gawlik, F. Gay-Balmaz, A finite element method for MHD that preserves energy, cross-helicity, magnetic helicity, incompressibility, and $\operatorname{div} \cdot \mathbf{B} = 0$, *Journal of Computational Physics* 450 (2022) 110847.
- [13] E. Hairer, C. Lubich, G. Wanner, *Geometric numerical integration: structure-preserving algorithms for ordinary differential equations*, Vol. 31, Springer Science & Business Media, 2006.
- [14] J. Kreeft, A. Palha, M. Gerritsma, Mimetic framework on curvilinear quadrilaterals of arbitrary order, arXiv:1111.4304 (2011) 69.
- [15] Y. Zhang, Mimetic spectral element method and extensions toward higher computational efficiency (2022).
- [16] P. Knupp, S. Steinberg, *Fundamentals of grid generation*, CRC press, 2020.
- [17] B. Sanderse, Energy-conserving Runge–Kutta methods for the incompressible Navier–Stokes equations, *Journal of Computational Physics* 233 (2013) 100–131.
- [18] H. Clercx, C.-H. Bruneau, The normal and oblique collision of a dipole with a no-slip boundary, *Computers & Fluids* 35 (3) (2006) 245–279. doi:<https://doi.org/10.1016/j.compfluid.2004.11.009>.
- [19] G. H. Golub, J. H. Welsch, Calculation of Gauss quadrature rules, *Mathematics of computation* 23 (106) (1969) 221–230.